IEEE Access
Multidisciplinary ⋮ Rapid Review ⋮ Open Access Journal

Received 31 October 2023, accepted 8 December 2023, date of publication 13 December 2023,
date of current version 18 December 2023.

Digital Object Identifier 10.1109/ACCESS.2023.3342199

RESEARCH ARTICLE

Position and Orientation Estimation in Radio Network With Groups of Locally Synchronized Nodes

JAROSLAW SADOWSKI AND JACEK STEFANSKI, (Member, IEEE)
Faculty of Electronics, Telecommunications and Informatics, Gdańsk University of Technology, 80-233 Gdańsk, Poland
Corresponding author: Jaroslaw Sadowski (jaroslaw.sadowski@eti.pg.edu.pl)

ABSTRACT This article presents a positioning system with groups of locally synchronized nodes. A mobile object is equipped with a group of several synchronized receivers that are able to measure the difference in the time of arrival of signals from reference transmitters. The reference transmitters are synchronized only in local groups, with no global synchronization between groups. It is assumed that the synchronous operation of transmitters and receivers in groups does not allow for the phase-coherent emission and reception of signals, making beamforming and angle of arrival estimation impossible. The structure of the positioning system and the equations for estimating the position and orientation angle are presented, along with the Gauss-Newton algorithm for iteratively estimating the coordinates and orientation of the mobile object. The possible accuracy of the proposed solution is evaluated using dilution of precision and the Cramer-Rao lower bound. The analysis showed that although the quality of the position estimation in the proposed solution is highly dependent on the mutual location of the reference transmitters and the mobile object, the orientation angle can be estimated highly accurately, almost regardless of the mobile object location.

INDEX TERMS Asynchronous positioning, Cramer-Rao lower bound, Gauss-Newton algorithm, radio localization, radio navigation.

I. INTRODUCTION

Radio positioning systems and networks can be divided into two groups. The first group includes positioning methods and techniques that do not require strict geometric relationships between the nodes to be determined, such as distances or bearing angles. Systems and solutions based on channel state information, neighborhood detection and fingerprinting (''range-free positioning'') are gaining a lot of attention [1], [2], [3], [4]. However, in most cases, these methods are designed for use in indoor environments only [5], [6] and are often designed to fit a specific scenario, without the possibility of generalization. On the other hand, radio-based positioning in outdoor environments, such as positioning in cellular networks, is still mainly performed using measurements of the geometric parameters of the radio network. Thus, the second group of positioning systems, which can be called ''range-based positioning'', is mostly based on measuring the time and the time difference between the radio signals received. As the size of the positioning system's area of operation increases, so does the number of reference stations and/or the distances between them. This makes it difficult to synchronize all base stations, which is necessary in most positioning methods based on one-way range estimation using time measurements. Two-way range measurement, on the other hand, requires mobile objects to be equipped with two-way communication devices (transmitting and receiving) which complicates the node structure and potentially creates system capacity limitations due to the need for multiple nodes to share the same radio resources. This has made researchers interested in the possibility of building radio localization networks that can estimate the positions of mobile nodes without needing to synchronize the operation of the reference stations.

The associate editor coordinating the review of this manuscript and approving it for publication was Sotirios Goudos.

An asynchronous TDoA positioning method was proposed in the PhD dissertation [7] and publication [8], in which reference nodes work in pairs. The first reference node transmits a positioning signal, which is received by the second reference node to determine the reference time, and by the mobile object, which must retransmit it to the second reference node. Although all reference nodes and mobile nodes can be clocked without synchronization in this solution, mobile objects must be equipped with a receiver and transmitter, which places limits on the system capacity.

Two-way communication is also assumed in another system, described in [9]. In this solution, all the reference nodes and the mobile nodes are clocked asynchronously, but all of them must be equipped with transmitting and receiving hardware. Signals received by reference nodes from other reference nodes are used to estimate clock bias.

In some ideas presented in the literature as asynchronous positioning, it is difficult to really consider it as asynchronous when the time offset between the free-running clocks at different nodes is explicitly measured and/or estimated from measurements before performing the position estimation. An example of such a case can be found in [10] and [11], where an additional signal from one reference node is used to measure the clocking difference in the second reference node. The solution presented in [12] uses the round-trip time principle to estimate the unknown time difference between reference nodes, which are then able to perform TDoA measurements. In another paper, [13], the asynchronous positioning problem is actually reduced to the problem of wireless synchronization of two separate subsets of reference nodes, both of which are locally synchronized. In yet another solutions proposed in [14] and [15], all anchor nodes are described as operating asynchronously, but after receiving a packet initiating the position estimation process from the primary node, they all have to send their positioning packets at a defined point in time. Therefore, the signals from all the reference nodes are sent in a synchronized manner and the position equations correspond to the classical synchronous TDoA system. Also, in [16], the positioning system is called asynchronous but uses the emission of signals with carrier synchronization, while the asynchronous position estimation method presented in [17] uses synchronized transmitters and estimation of the unknown transmission time in mobile receivers. However, in [18], the unknown times of fully asynchronous emissions of positioning signals are removed from the equations using double differential measurement, making it a truly asynchronous system. Thus, the classification of various systems as asynchronous is not precise.

In this article, devices (transmitters, receivers) will be called synchronous when they are clocked in such a way that all time dependencies regarding their tasks (time of emission, time of radio signal reception) are strictly defined and repeatable and can be expressed in relation to one reference time moment. On the other hand, asynchronous devices are clocked by independent clocks, so the timing relationships between their tasks (transmission, reception of radio signals) can only be defined and maintained within single device, but not between different devices. Therefore, a common time scale for asynchronous devices cannot be defined.

In addition to the position of mobile objects, the orientation of these objects relative to a specific reference direction can also be important in some applications. Joint position and orientation estimation in a radio network was presented in [19] and [20]. In these articles, channel state information, delay and angle of arrival estimation is performed using linear antenna arrays working with OFDM signals. Despite promising results, the proposed solution requires coherent signal processing across antenna arrays. An interesting method for measuring the relative position and orientation of two freight containers was proposed in [21]. In this solution, two DW1000 ultrawideband modules are installed on each container and they measure four distances using the round-trip time method. The results of the measurements are then used to estimate the displacement and rotation angle of the second container relative to the first one. In addition, the article [22] contains the results of a study on the relative positioning of robots with a more sophisticated configuration of four UWB sensors. The mobile robots are able to measure the distances using the RTT method, but the results of the measurements are weighted to reduce the impact of less accurate range data collected using obstructed antennas.

In this article, a positioning system is proposed that addresses both of the aforementioned research topics: estimating the position and orientation angle of a mobile object using time-based measurements in a partially synchronized network. In this solution, the mobile object is equipped with a set of synchronized receivers, but fixed reference nodes operate synchronously only in local groups, while global synchronization of all transmitters is not necessary. One possible application area for the proposed system structure is aviation. The dimensions of commercial aircraft are large enough to consider installing two or more synchronized receivers on them. A good place to install the reference nodes for plane tracking is the tops of wind turbine towers, which are usually tall and located in open terrain. Wind turbines are placed in groups to form wind farms, and the distances between neighboring turbines are in the order of hundreds of meters, which makes it possible to achieve synchronization of the timing of signal emissions, for example, using direct cabling, but large distances between neighboring wind farms significantly hinders the construction of a fully synchronous network, so only local synchronization of transmitters within wind farms can be justified.

The rest of the article is organized as follows: Section II-A presents the basic structure of the position and orientation angle estimation system with one group of synchronized base stations, and the general structure of the system with multiple groups of transmitters is presented in section II-B. The third section contains the results of simulations estimating the position and orientation angle, together with the Cramer-Rao

lower bound. Finally, a conclusion is given in the fourth section, with a discussion on possible applications of the proposed position and orientation angle estimation method.

II. STRUCTURE OF SYSTEM FOR POSITION AND ORIENTATION ESTIMATION

Consider a two-dimensional (2D) environment in which mobile objects are present, whose positions and orientations with respect to a fixed reference direction must be estimated. The positioning system consists of set of fixed base stations acting as reference nodes for distance difference measurements and set of mobile nodes attached to the tracked object. As the distance between the reference nodes increases, precise synchronization of devices becomes more challenging. Therefore, to simplify the network construction, nearby base stations are arranged in groups and only the stations within each group are synchronized, while different groups of stations, usually located at greater distances, operate asynchronously. Further in the article, it will be assumed that base stations (reference nodes) are transmitting positioning signals. The tracked object is equipped with a set of synchronized receivers that are able to measure the time difference between the receipt of signals from different transmitters by the same receiver, but also the reception time of signals from the same transmitter by different receivers and signals from different transmitters arriving at different receivers. In contrast to the network structure presented in [23], a variable number of nodes on the tracked object will be considered. Thus, in the proposed system structure, the groups of locally synchronized nodes are: separate groups of reference transmitters in stationary base stations and one group of mobile receivers located on the tracked object. The reverse configuration – groups of base stations with synchronized fixed reference receivers and a mobile object equipped with a set of synchronized transmitters – is also possible but the case with fixed reference transmitters is preferred because it allows for unlimited system capacity. It is also assumed that the synchronization of the base stations in groups and the synchronization of the mobile nodes deployed on the tracked object does not allow the creation of any beamforming, neither on the transmitting nor receiving side, which may be caused, for example, by non-coherent carrier generation in all devices. Time difference measurements are therefore the only measurements possible in the system under consideration.

A. ONE GROUP OF SYNCHRONIZED REFERENCE NODES

The mobile object, whose position and orientation is to be estimated, is equipped with N synchronized receivers. The mobile object has a defined reference point for expressing its coordinates and reference orientation axis for expressing its orientation angle. Thus, the position of the n^{th} receiver can be expressed as x^0_{rn}, y^0_{rn}, which are coordinates in a local coordinate system associated with the tracked object, with the origin at the object's reference point and the "Y" axis aligned with the object's orientation axis, as presented in Fig. 1.

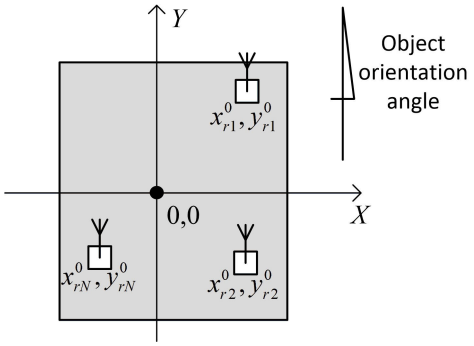

FIGURE 1. Local coordinate system associated with the tracked object.

In the simplest scenario, there is only one group of M synchronized reference transmitters, deployed over limited area due to some unspecified constraints on the maximum distance of the transmitters' synchronization. The general geometry of the positioning system is shown in Fig. 2. Therefore, this can be understood as a generalization of the positioning method proposed in [21] and [22] with the important difference being that it measures distance differences instead of estimating the distances using RTT on UWB.

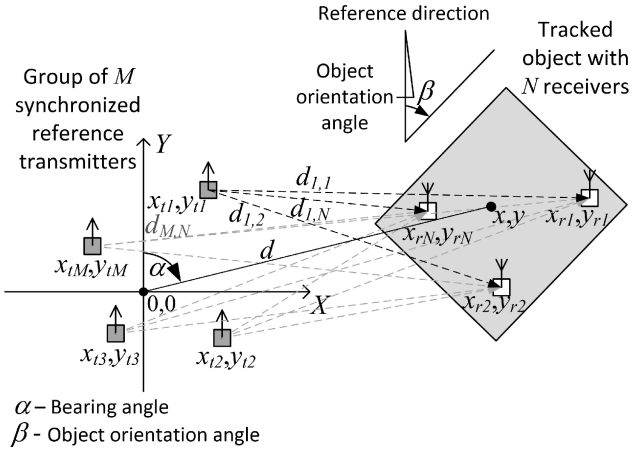

FIGURE 2. Geometry of positioning system with one group of synchronized reference transmitters.

In the global, fixed coordinate system, the coordinates of the n^{th} receiver on the mobile object located at point (x,y) and rotated by angle β are calculated from the local coordinates x^0_{rn}, y^0_{rn} using:

$$x_{rn} = x + x^0_{rn} \cdot \cos(\beta) + y^0_{rn} \cdot \sin(\beta) \quad (1)$$

$$y_{rn} = y + y^0_{rn} \cdot \cos(\beta) - x^0_{rn} \cdot \sin(\beta) \quad (2)$$

Synchronized receivers are able to measure the difference in time of arrival of signals from all transmitters, either emitted at the same time or sequentially. However, the technical implementation of both transmission and reception of these signals is beyond the scope of this article. Denoting the receipt time of the signal from the m^{th} transmitter by the n^{th}

receiver as $t_{rm,n}$, the results of the measurements are:

$$\left(t_{rm_2,n_2} - t_{rm_1,n_1}\right) = \left(t_{tm_2} + \frac{d_{m_2,n_2}}{v}\right) - \left(t_{tm_1} + \frac{d_{m_1,n_1}}{v}\right) + \varepsilon_{m_2,n_2,m_1,n_1} \quad (3)$$

where m_2, n_2 and m_1, n_1 are identifiers of the transmitters (m_1, m_2) whose signals are being measured and the receivers (n_1, n_2) used to receive these signals and estimate the time difference of arrival $\left(t_{rm_2,n_2} - t_{rm_1,n_1}\right)$, and $\varepsilon_{m_2,n_2,m_1,n_1}$ is measurement error, later modelled in simulations as Gaussian random variable. The measurements of t_{rm_2,n_2} and t_{rm_1,n_1} are taken with reference to the local clock in the receivers, not synchronized with the transmission time, therefore only differential measurements can be used for positioning. The values t_{tm_1}, t_{tm_2} are the time of emission of the signals from transmitters m_1 and m_2, respectively, whose absolute values are unknown but the difference $(t_{tm_2} - t_{tm_1})$ is known due to the synchronous work of all the transmitters in the group and so can be subtracted from the equations. Therefore, from the measurements defined in equation (3), the difference $\left(d_{m_2,n_2} - d_{m_1,n_1}\right)$ between the distance from transmitter m_1 to receiver n_1 and the distance from transmitter m_2 to receiver n_2 can be calculated, which leads to the following positioning equation:

$$\left(d_{m_2,n_2} - d_{m_1,n_1}\right) = \sqrt{\left(x_{rn_2} - x_{tm_2}\right)^2 + \left(y_{rn_2} - y_{tm_2}\right)^2} - \sqrt{\left(x_{rn_1} - x_{tm_1}\right)^2 + \left(y_{rn_1} - y_{tm_1}\right)^2} \quad (4)$$

where x_{rn_1}, y_{rn_1}, x_{rn_2}, y_{rn_2} are calculated using (1) and (2) and contain both the unknown coordinates (x, y) and the orientation angle (β). Calculating the set of equations (4) for at least three combinations of transmitters and receivers makes it possible to estimate both the position of the mobile object (x, y) and it's orientation angle β, as long as at least two transmitters and at least two receivers are used in the measurements. If only one receiver is used, it is not possible to estimate the orientation angle and (4) represents classic TDoA hyperbolic positioning. However, in case of one transmitter only, the results of distance difference measurements are the same for every possible bearing angle α, so the system of equations (4) becomes indeterminate, and therefore unambiguous position or orientation estimation is not possible for any number of receivers.

The quality of position estimation using (4) depends on the distance between the tracked object and the group of reference nodes, even if the accuracy of the distance difference measurements remains unchanged. On the other hand, the quality of the orientation angle estimation using (4) is distance-independent, as long as measurement error characteristics are kept constant. Therefore, the proposed system geometry is especially suitable for applications where only the orientation of the tracked object matters. It can be shown that for a mobile object at a large distance from the group of reference nodes, object orientation angle β can be calculated by simplified equations:

$$\begin{aligned}\left(d_{m_2n_2} - d_{m_1n_1}\right) = &\left[\left(x^0_{rn_2}\cos\beta + y^0_{rn_2}\sin\beta\right)\right. \\ &\left. - \left(x_{tm_2}\cos\alpha + y_{tm_2}\sin\alpha\right)\right] \\ &- \left[\left(x^0_{rn_1}\cos\beta + y^0_{rn_1}\sin\beta\right)\right. \\ &\left. - \left(x_{tm_1}\cos\alpha + y_{tm_1}\sin\alpha\right)\right] \end{aligned} \quad (5)$$

The α symbol denotes the bearing angle to the tracked object from the group of reference nodes, illustrated in Fig. 2. The systematic errors caused by the approximation that all measurements are made along parallel directions decreases with the increasing distance. Differences between orientation angle estimation errors obtained using exact equations (4) and approximation (5) will be presented in Section III-A.

B. GENERAL STRUCTURE OF SYSTEM WITH INDEPENDENT GROUPS OF SYNCHRONIZED NODES

The deployment of several groups of locally synchronized base stations over a defined area, which is larger than the constraints on the ability to synchronize base stations, gives the structure of the positioning system shown in the block diagram in Fig. 3.

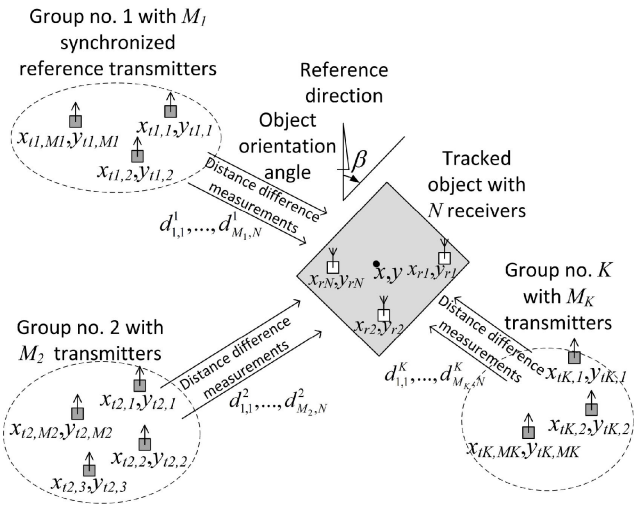

FIGURE 3. Block diagram of 2D position and orientation estimation system with groups of synchronized nodes.

The tracked object is still equipped with N synchronous receivers. However, the fixed infrastructure is divided into K groups of base stations with locally synchronized transmitters. The number M_k of transmitters in the k^{th} group ($k = 1 \ldots K$) can vary, as can the spatial distribution of transmitters in the group. In the case of $K = 1$, $N = 1$, the classical hyperbolic system based on TDoA measurements is obtained, while $N = 2$ and $M_k = 1$ for any $k = 1 \ldots K$ results in position and orientation estimation equations (4) equivalent to the system structure presented in [23]. Please note that in this system structure, the number of simultaneously tracked objects is also not limited to one.

Position and orientation estimation in the system presented in Fig. 5 is performed using the system of equations (4) defined earlier for a system configuration with all transmitters working synchronously. When the base stations are divided into separate groups that cannot maintain synchronization between them, the only additional restriction is to not mix measurement data obtained from signals emitted by transmitters from different groups in the same equation (4).

The system of equations (4) can be solved iteratively using, e.g., the Gauss-Newton algorithm [24], [25]. Estimates of all the unknown variables are presented in the vector:

$$\mathbf{x}_i = \begin{bmatrix} \hat{x}_i \\ \hat{y}_i \\ \hat{\beta}_i \end{bmatrix}, \tag{6}$$

where i denotes the i^{th} step of the iterative estimation. Matrix $\mathbf{J}$ is a Jacobian matrix containing partial derivatives of (4) with respect to all the unknown variables, calculated at the current position and orientation estimates in the i^{th} step:

$$\mathbf{J}_i = \begin{bmatrix} j_{i,1,1} & j_{i,1,2} & j_{i,1,3} \\ \vdots & \vdots & \vdots \\ j_{i,(m1,n1,m2,n2),1} & j_{i,(m1,n1,m2,n2),2} & j_{i,(m1,n1,m2,n2),3} \\ \vdots & \vdots & \vdots \end{bmatrix}. \tag{7}$$

Rows of (7) are defined for any pair of transmitter (m_1, m_2) and receiver (n_1, n_2) identifiers for which measurements are taken:

$$j_{i,(m_1,n_1,m_2,n_2),1} = \frac{\hat{x}_{i,rn_2} - x_{tm_2}}{\sqrt{\left(\hat{x}_{i,rn_2} - x_{tm_2}\right)^2 + \left(\hat{y}_{i,rn_2} - y_{tm_2}\right)^2}} - \frac{\hat{x}_{i,rn_1} - x_{tm_1}}{\sqrt{\left(\hat{x}_{i,rn_1} - x_{tm_1}\right)^2 + \left(\hat{y}_{i,rn_1} - y_{tm_1}\right)^2}} \tag{8}$$

$$j_{i,(m_1,n_1,m_2,n_2),2} = \frac{\hat{y}_{i,rn_2} - y_{tm_2}}{\sqrt{\left(\hat{x}_{i,rn_2} - x_{tm_2}\right)^2 + \left(\hat{y}_{i,rn_2} - y_{tm_2}\right)^2}} - \frac{\hat{y}_{i,rn_1} - y_{tm_1}}{\sqrt{\left(\hat{x}_{i,rn_1} - x_{tm_1}\right)^2 + \left(\hat{y}_{i,rn_1} - y_{tm_1}\right)^2}} \tag{9}$$

$$j_{i,(m_1,n_1,m_2,n_2),3} = \frac{\left(y^0_{rn_2}\left(y_{tm_2} - \hat{y}_i\right) + x^0_{rn_2}\left(x_{tm_2} - \hat{x}_i\right)\right)\sin\hat{\beta}_i}{\sqrt{\left(\hat{x}_{i,rn_2} - x_{tm_2}\right)^2 + \left(\hat{y}_{i,rn_2} - y_{tm_2}\right)^2}} + \frac{\left(x^0_{rn_2}\left(y_{tm_2} - \hat{y}_i\right) - y^0_{rn_2}\left(x_{tm_2} - \hat{x}_i\right)\right)\cos\hat{\beta}_i}{\sqrt{\left(\hat{x}_{i,rn_2} - x_{tm_2}\right)^2 + \left(\hat{y}_{i,rn_2} - y_{tm_2}\right)^2}} - \frac{\left(y^0_{rn_1}\left(y_{tm_1} - \hat{y}_i\right) + x^0_{rn_1}\left(x_{tm_1} - \hat{x}_i\right)\right)\sin\hat{\beta}_i}{\sqrt{\left(\hat{x}_{i,rn_1} - x_{tm_1}\right)^2 + \left(\hat{y}_{i,rn_1} - y_{tm_1}\right)^2}} - \frac{\left(x^0_{rn_1}\left(y_{tm_1} - \hat{y}_i\right) - y^0_{rn_1}\left(x_{tm_1} - x_i\right)\right)\cos\hat{\beta}_i}{\sqrt{\left(\hat{x}_{i,rn_1} - x_{tm_1}\right)^2 + \left(\hat{y}_{i,rn_1} - y_{tm_1}\right)^2}} \tag{10}$$

where $\hat{x}_{i,rn_1}, \hat{y}_{i,rn_1}, \hat{x}_{i,rn_2}, \hat{y}_{i,rn_2}$ are defined as:

$$\hat{x}_{i,rn} = \hat{x}_i + x^0_{rn}\cos\hat{\beta}_i + y^0_{rn}\sin\hat{\beta}_i, \tag{11}$$

$$\hat{y}_{i,rn} = \hat{y}_i + y^0_{rn}\cos\hat{\beta}_i - x^0_{rn}\sin\hat{\beta}_i. \tag{12}$$

Defining vector $\mathbf{z}$ of the differences between the results of the measurements and the current estimates of the distance difference values:

$$\mathbf{z}_i = \begin{bmatrix} z_{i,1} \\ \vdots \\ z_{i,(m_1,n_1,m_2,n_2)} \\ \vdots \end{bmatrix} \tag{13}$$

$$z_{i,(m_1,n_1,m_2,n_2)} = \left(d_{m_2,n_2} - d_{m_1,n_1}\right) - \sqrt{\left(\hat{x}_{i,rn_2} - x_{tm_2}\right)^2 + \left(\hat{y}_{i,rn_2} - y_{tm_2}\right)^2} + \sqrt{\left(\hat{x}_{i,rn_1} - x_{tm_1}\right)^2 + \left(\hat{y}_{i,rn_1} - y_{tm_1}\right)^2} \tag{14}$$

an update vector $\boldsymbol{\delta}$ can be calculated:

$$\boldsymbol{\delta}_i = \left(\mathbf{J}_i^T\mathbf{R}^{-1}\mathbf{J}_i\right)^{-1}\mathbf{J}_i^T\mathbf{R}^{-1}\mathbf{z}_i \tag{15}$$

where $\mathbf{R}$ is a measurements covariance matrix. The elements of $\mathbf{R}$ take value σ_d^2 on the diagonal, $\sigma_d^2/2$ in the elements corresponding to equations (4) which use the same set of transmitter (m) and receiver (n) indices in d_{m_1,n_1} or d_{m_2,n_2} and zero otherwise, where σ_d is the standard deviation of distance difference measurement error. Finally, the vector of the estimated coordinates and orientation angles is iteratively updated:

$$\mathbf{x}_{i+1} = \mathbf{x}_i + \boldsymbol{\delta}_i \tag{16}$$

The Gauss-Newton algorithm requires an initial position and orientation estimate for the first iteration. A badly chosen starting point can lead to algorithm divergence or convergence to incorrect final results, but the problem of selecting the starting point will not be discussed in detail here, as the reader may wish to use a different algorithm to solve the system of equations (4). However, it should be noted that the approximate estimation of object orientation using the system of equations (5), although it introduces some systematic bias into the results, is more robust in terms of convergence and can be used to roughly estimate β for the final position and orientation estimation using (4).

III. POSITION AND ORIENTATION ESTIMATION QUALITY

A. SYSTEM PERFORMANCE WITH ONE GROUP OF TRANSMITTERS

The structure of the positioning system with one group of M synchronized transmitters and one group of N synchronized mobile receivers used for simulations is shown in Fig. 4. All transmitters and all receivers are evenly distributed on two circles of equal radius r. To allow for scaling of the results, the radius r is also used to represent the distance of the mobile object from the origin and to characterize the errors of the distance difference measurements.

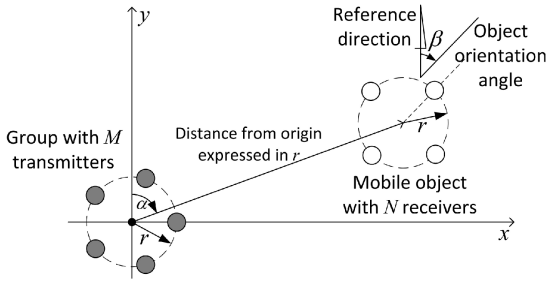

FIGURE 4. System geometry for simulating a case with one group of synchronized transmitters only.

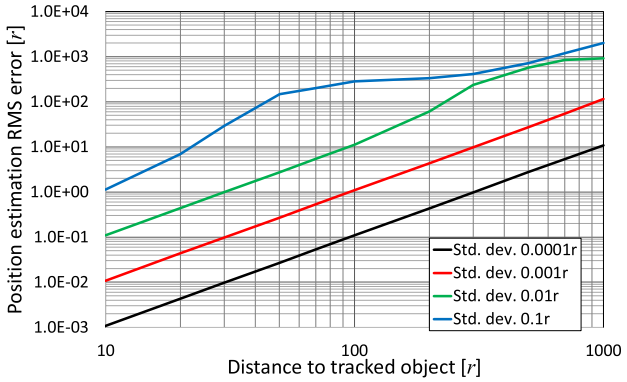

FIGURE 5. Position estimation error as a function of the distance to the tracked object and the standard deviation of the distance-differences measurement error, normalized to the radius r of the circles on which the transmitters and receivers are located. $M = 5$, $N = 4$.

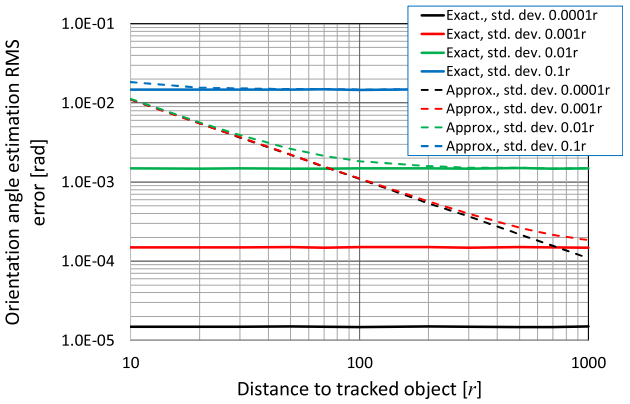

FIGURE 6. Orientation angle estimation error as a function of the distance to the tracked object and the standard deviation of the distance-differences measurement error, normalized to the radius r of the circles on which the transmitters and receivers are located. $M = 5$, $N = 4$.

The quality of position and orientation angle estimation was simulated in an example scenario with five reference transmitters and four receivers. Position estimation errors, shown in Fig. 5, are highly dependent on the distance of the mobile object from the transmitter group. During the simulation, it was assumed that the error $\varepsilon_{m_2,n_2,m_1,n_1}$ in the distance difference measurements is modeled in (3) as a sum of two Gaussian random variables $\varepsilon_{m_1,n_1} + \varepsilon_{m_2,n_2}$ corresponding to independent error of detection time t_{rm_1,n_1} and t_{rm_2,n_2} respectively and when the same transmitter number m and receiver number n occurs in (3), the same error values are added in simulation to model correlated measurement errors. Assuming that standard deviation of simulated distance difference error is σ_d, both time measurement error terms ε_{m_1,n_1} and ε_{m_2,n_2} are normal random variables with standard deviation equal $\sigma_d/(\sqrt{2}v)$. To simplify evaluation of results, σ_d is expressed as a fraction of r. However, it should be noted that for the simulations the measurement error characteristics were assumed to be distance-independent. Also, the distance from the set of transmitters to the tracked object is expressed in r, which simplifies the scaling of results for different system geometries. When the RMS position estimation error exceeds approx. $100r$, the iterative position estimation algorithm presented in Section II is not guaranteed to converge to correct results. Simulations leading to algorithm divergence have been excluded from the data shown in Fig. 5, but for large distances and large measurement errors, even converged results show some irregularities which partially depends on the adopted data exclusion criteria.

Comparing to position estimation, orientation angle calculation using exact equations (4) is almost distance-independent, as can be seen in Fig. 6 (solid lines). This chart shows the RMS error of the orientation angle estimate from the exact and approximate calculations using the same assumptions about the system geometry and structure that were used when simulating the position estimation error.

As it was expected, additional errors (dashed lines in Fig. 6) caused by the assumption that distance difference measurements are made along perpendicular lines and by using approximate equations (5) decrease as the distance between the tracked object and the group of transmitters increases.

B. DILUTION OF PRECISION

The accuracy of estimation of the location and/or orientation parameters in almost any radiolocation system depends not only on the quality of the measurements of the parameters of the radio signals but also on the form of the position calculation equations and the mutual distribution of the nodes that are involved in the positioning. A good indicator of the system's susceptibility to measurement error is a parameter called dilution of precision (*DOP*), which is widely used in the analysis of satellite positioning systems [26], [27], [28] but can also be used to characterize other solutions based on geometric dependencies [29]. The *DOP* coefficient indicates the ratio of the estimation error of the unknown parameters (position, orientation) observed in the analyzed system to the error of the measurements performed [30], [31]. Knowing the Jacobian matrix $\mathbf{J}$, the *DOP* parameters can be easily estimated from the values of the elements on the diagonal of the matrix $\mathbf{Q}$:

$$\mathbf{Q} = \left(\mathbf{J}^T \cdot \mathbf{J}\right)^{-1} \tag{17}$$

In our case, the first and second columns of matrix J contain partial derivatives of equation (4) with respect to the x and y coordinates, respectively, therefore the position dilution of precision (*PDOP*) parameter is defined as:

$$PDOP = \sqrt{\mathbf{Q}_{1,1} + \mathbf{Q}_{2,2}} \tag{18}$$

Also, the third element on the diagonal of $\mathbf{Q}$ makes it possible to define the orientation angle (direction) dilution of precision (*DDOP*) parameter:

$$DDOP = \sqrt{\mathbf{Q}_{3,3}} \tag{19}$$

The distance difference measurement error, which can be expressed in various units of distance, transfers onto the orientation angle error, which in equation (4) is always in radians. Therefore, the *DDOP* values will depend on the selected units of distance.

In the proposed system, the *DOP* parameters depend on many factors, such as the number of transmitter groups K, the number of transmitters in each group M_k, the number of receivers on the mobile object N, and the spatial distribution of the groups, transmitters in the groups and receivers. Such a variety of possible system configurations under consideration makes it difficult to analyze and present the quality of position and orientation estimation, making some simplifications necessary. Firstly: all the N receivers on the tracked object and all transmitters in all groups are evenly distributed on circles of the same radius r. Groups of synchronized transmitters are evenly spaced over a larger circle of radius R. The number of groups K is variable, and each group contains a variable but equal number of transmitters $M_k = M$ for each $k = 1 \ldots K$. The selected system structure for the *DOP* study is shown in Fig. 7.

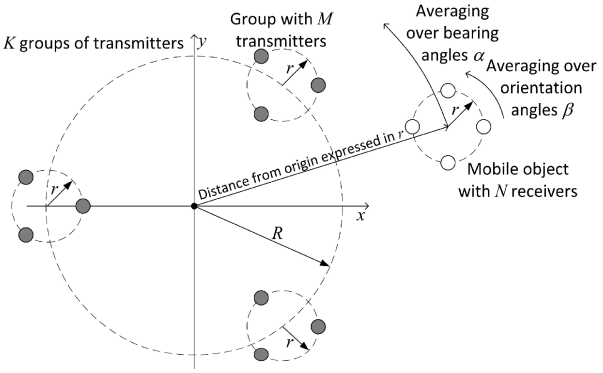

FIGURE 7. General structure of positioning system for DOP investigation.

The graphs in Figures 8–15 show the position and orientation angle dilution of precision as a function of the distance of the mobile object from the origin defined in the center of the circle of transmitter groups. To simplify the scaling of the results, the mobile object distance and the radius of the larger circle R were expressed as a multiple of the smaller circle radius r and the results are shown for three different values of $R = 10r$, $R = 30r$ and $R = 100r$. For the

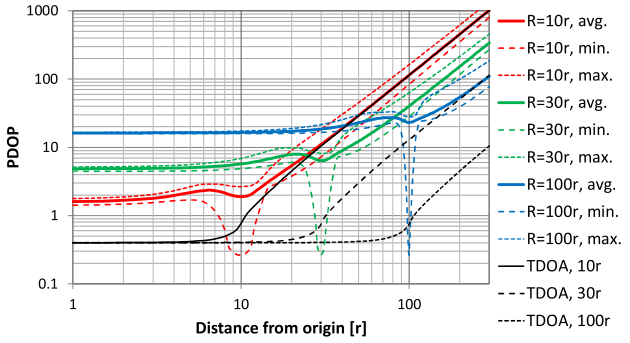

FIGURE 8. PDOP in a system with $K = 3$ groups of transmitters, $M = 3$ transmitters in each group, $N = 3$ receivers in the mobile object.

PDOP investigation, some spread of results was observed for different bearing and orientation angles of the mobile object at the same distance from the origin, so in addition to the average *PDOP* for all bearing and orientation angles, the minimum and maximum *PDOP* values are also shown. Significant reduction in the minimum *PDOP* values occurring at distances close to the radius of the large circle R is caused by the fact that during averaging *PDOP* results for different orientation angles α, for some of them the tracked object is located very close to one of the transmitter groups, closer than at any other position. Short distances between transmitters and receivers in such a case increase the differences between the orientation angles of lines connecting connect all transmitter-receiver pairs involved in position estimation, which reduces the impact of measurement errors on the final position estimation quality. Additionally, reference results of *PDOP* simulation for a fully synchronous TDoA system with five base stations evenly spaced on a circle of radius R are also shown in Figures 8-11 to simplify the comparison of synchronous and partially synchronous positioning. With classical TDoA positioning, the mobile object is equipped with only one receiver, therefore orientation estimation in the reference system was not possible.

The graphs in Figures 12–15 show the orientation angle dilution of precision. Unlike the *PDOP*, the results the of *DDOP* investigation were almost independent of the object orientation, so only average values are presented. But it is important to note that in the simulated scenario, the results of the *DDOP* estimation correspond to the ratio of the orientation angle estimation error expressed in radians to the distance difference measurement error normalized to the radius of the smaller circle r.

The first set of graphs in Figures 8 and 12 shows *DOP* simulation results for the system configuration with three groups of three synchronized transmitters and three synchronized receivers on the tracked object. Although this is not the minimum useful configuration of the proposed system, which in most cases can provide position and orientation estimation even for smaller configurations (e.g. $K = 1$, $M = 3$, $N = 2$), reducing the number of nodes can cause large irregularities in the *DOP* distribution and can cause the

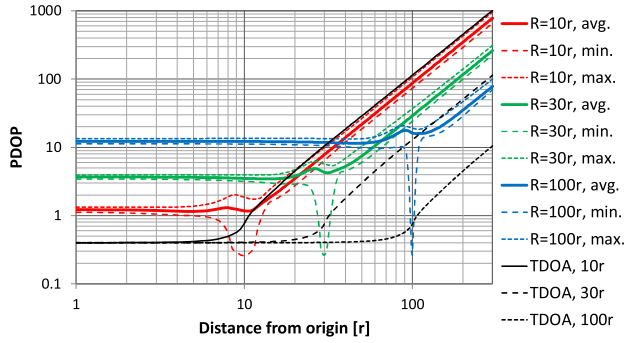

FIGURE 9. PDOP in a system with $K = 5$ groups of transmitters, $M = 3$ transmitters in each group, $N = 3$ receivers in the mobile object.

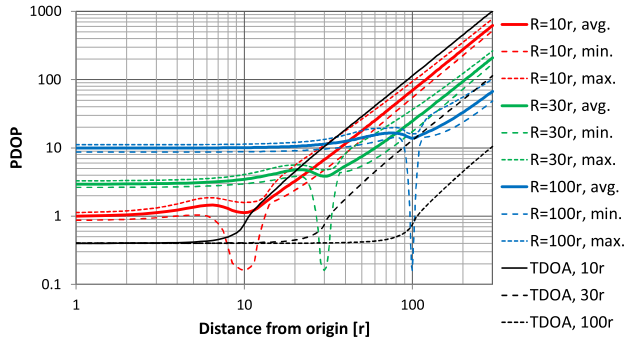

FIGURE 10. PDOP in a system with $K = 3$ groups of transmitters, $M = 5$ transmitters in each group, $N = 3$ receivers in the mobile object.

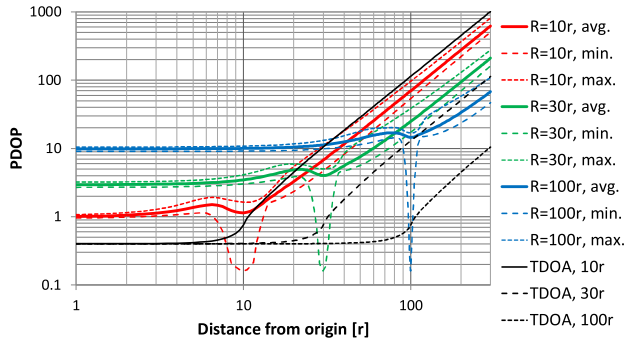

FIGURE 11. PDOP in a system with $K = 3$ groups of transmitters, $M = 3$ transmitters in each group, $N = 5$ receivers in the mobile object.

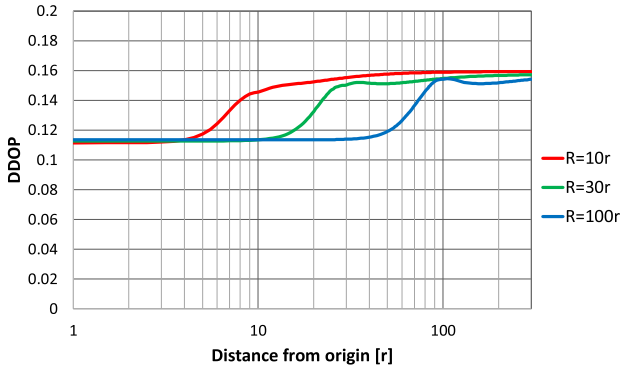

FIGURE 12. DDOP in a system with $K = 3$ groups of transmitters, $M = 3$ transmitters in each group, $N = 3$ receivers in the mobile object.

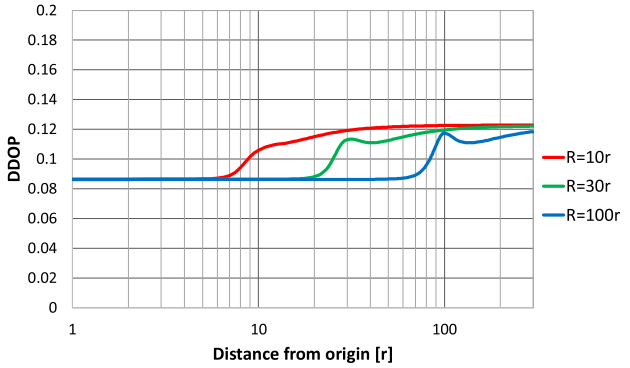

FIGURE 13. DDOP in a system with $K = 5$ groups of transmitters, $M = 3$ transmitters in each group, $N = 3$ receivers in the mobile object.

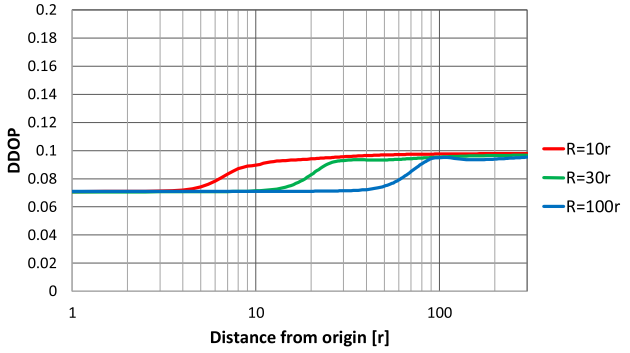

FIGURE 14. DDOP in a system with $K = 3$ groups of transmitters, $M = 5$ transmitters in each group, $N = 3$ receivers in the mobile object.

Gauss-Newton algorithm to diverge. The next graphs show *DOP* simulation results for system configurations with more transmitter groups (Figures 9 and 13), more transmitters in each group (Figures 10 and 14) and more receivers on the tracked object (Figures 11 and 15). Changing only one system parameter in each simulation makes it easier to assess the impact of the given parameter on the quality of the position and orientation estimation.

The presented results clearly show that inside the region surrounded by groups of transmitters, the average *PDOP* value is almost position-independent, which is a huge advantage of a system with several groups of locally synchronized base stations over the variant with a single group of reference stations. Outside the large circle area, the position dilution of precision parameter increases with the distance of the mobile object from the origin but comparing the *PDOP* curves obtained for the proposed system with the classical TDoA system, it can be seen that the rate of *PDOP* increase is comparable to that observed in synchronous hyperbolic positioning network. The simulations show that, although any increase in the total number of nodes involved in position estimation leads to a reduction in *PDOP*, a greater improvement can be observed when increasing the number of receivers or

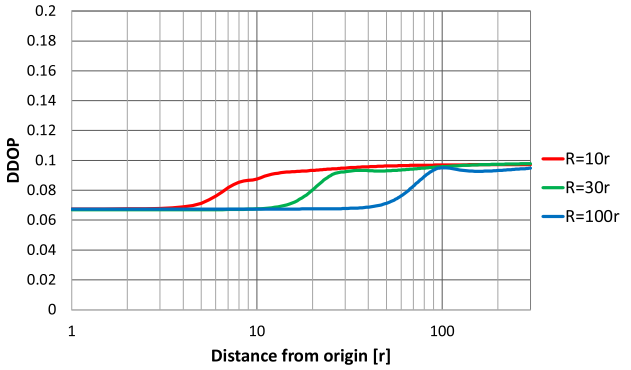

FIGURE 15. DDOP in a system with $K = 3$ groups of transmitters, $M = 3$ transmitters in each group, $N = 5$ receivers in the mobile object.

the number of transmitters in groups than when increasing the number of groups with no change in group size.

Compared to position estimation, the quality of orientation angle estimation in the proposed system is only slightly affected by the position of the mobile object inside and outside the large circle in the scenario presented in Fig. 7. The greatest variation in *DDOP* values is seen in Figs. 12 and 13, but the increase in *DDOP* as the distance of the mobile object from the origin increases is limited to only 42% compared to the lowest *DDOP* in the origin. This confirms the suitability of the proposed solution for estimating the orientation of objects whose size allows them to be equipped with a set of synchronized nodes (receivers) of the localization system.

C. CRAMER-RAO BOUND

The Cramer-Rao lower bound (CRLB) is commonly used to assess how accurate estimates of unknown, but deterministic parameter can be obtained using certain estimation methods [32]. This parameter defines the minimum mean square error of an unbiased estimator $\hat{\boldsymbol{\theta}}$ of unknown vector $\boldsymbol{\theta}$ as:

$$\text{var}\left(\hat{\boldsymbol{\theta}}\right) \geq \mathbf{I}(\boldsymbol{\theta})^{-1} \tag{20}$$

where the matrix:

$$\mathbf{I}(\boldsymbol{\theta}) = -E\left[\frac{\partial^2 \ln p(\boldsymbol{\rho};\boldsymbol{\theta})}{\partial \boldsymbol{\theta}^2}\right] \tag{21}$$

is called a Fisher information matrix. Function $p(\boldsymbol{\rho};\boldsymbol{\theta})$ is a conditional probability density function of the measurement vector ρ given θ. In our case, the vector ρ contains all results of distance difference measurements:

$$\boldsymbol{\rho} = \begin{bmatrix} d_{1,2} - d_{1,1} \\ \vdots \\ d_{m_2,n_2} - d_{m_1,n_1} \\ \vdots \end{bmatrix} \tag{22}$$

and the estimated vector θ has three elements: two coordinates in the Cartesian coordinate system and an orientation angle:

$$\boldsymbol{\theta} = \begin{bmatrix} x \\ y \\ \beta \end{bmatrix} \tag{23}$$

Assuming a Gaussian distribution of measurement error:

$$p(\boldsymbol{\rho};\boldsymbol{\theta}) = \frac{1}{\sqrt{2\pi\sigma^2}} \exp\left[-\frac{1}{2\sigma^2}\left|\boldsymbol{\rho} - f(\boldsymbol{\theta})\right|^2\right] \tag{24}$$

where $f(\boldsymbol{\theta})$ is a function that combines the estimated values and measurement results, derived from equation (4). After substituting (4) and (22) the conditional probability function takes the form:

$$p(\boldsymbol{\rho};\boldsymbol{\theta}) = \frac{1}{\sqrt{2\pi\sigma^2}} \exp\left\{-\frac{1}{2\sigma^2} \sum_{m_1,m_2,n_1,n_2} \left[\left(d_{m_2,n_2} - d_{m_1,n_1}\right) - \left(\sqrt{\left(x_{rn_2} - x_{tm_2}\right)^2 + \left(y_{rn_2} - y_{tm_2}\right)^2} - \sqrt{\left(x_{rn_1} - x_{tm_1}\right)^2 + \left(y_{rn_1} - y_{tm_1}\right)^2}\right)\right]^2\right\} \tag{25}$$

The Fisher information matrix is then defined as:

$$\mathbf{I}(\boldsymbol{\theta}) = \begin{bmatrix} -E\frac{\partial^2 \ln p(\boldsymbol{\rho};\boldsymbol{\theta})}{\partial x^2} & -E\frac{\partial^2 \ln p(\boldsymbol{\rho};\boldsymbol{\theta})}{\partial x \partial y} & -E\frac{\partial^2 \ln p(\boldsymbol{\rho};\boldsymbol{\theta})}{\partial x \partial \beta} \\ -E\frac{\partial^2 \ln p(\boldsymbol{\rho};\boldsymbol{\theta})}{\partial y \partial x} & -E\frac{\partial^2 \ln p(\boldsymbol{\rho};\boldsymbol{\theta})}{\partial y^2} & -E\frac{\partial^2 \ln p(\boldsymbol{\rho};\boldsymbol{\theta})}{\partial y \partial \beta} \\ -E\frac{\partial^2 \ln p(\boldsymbol{\rho};\boldsymbol{\theta})}{\partial \beta \partial x} & -E\frac{\partial^2 \ln p(\boldsymbol{\rho};\boldsymbol{\theta})}{\partial \beta \partial y} & -E\frac{\partial^2 \ln p(\boldsymbol{\rho};\boldsymbol{\theta})}{\partial \beta^2} \end{bmatrix} \tag{26}$$

and variances of the estimates of the position and orientation angle are bounded by inequalities:

$$\text{var}\left(\hat{x},\hat{y}\right) \geq \left[\mathbf{I}(\boldsymbol{\theta})^{-1}\right]_{1,1} + \left[\mathbf{I}(\boldsymbol{\theta})^{-1}\right]_{2,2} \tag{27}$$

$$\text{var}\left(\hat{\beta}\right) \geq \left[\mathbf{I}(\boldsymbol{\theta})^{-1}\right]_{3,3} \tag{28}$$

All the partial derivatives present in the matrix $\mathbf{I}(\boldsymbol{\theta})$ are shown in Appendix. Thus, the final form of the Fisher information matrix and the value of the CRLB depend on the position and orientation, so the easiest way to evaluate the limits of the quality of the position and orientation angle estimation is through numerical simulation. Therefore, the quality of the position and orientation angle estimation was simulated for the system with the structure presented in Section III.A during the analysis of the DOP parameter with the following assumptions: the tracked object is equipped with $N = 3$ receivers evenly distributed on a circle of radius r. Three sets of three synchronized transmitters ($M_k = 3$ for each $k = 1 \ldots 3$) are evenly distributed over a larger circle of radius R and the simulations were repeated for different ratios between R and r: $R = 10r$, $R = 30r$ and $R = 100r$. The averaged results of the Cramer-Rao bound and the variance of the position estimation error obtained using the Gauss-Newton algorithm are shown in Fig. 16, while Fig. 17 shows the

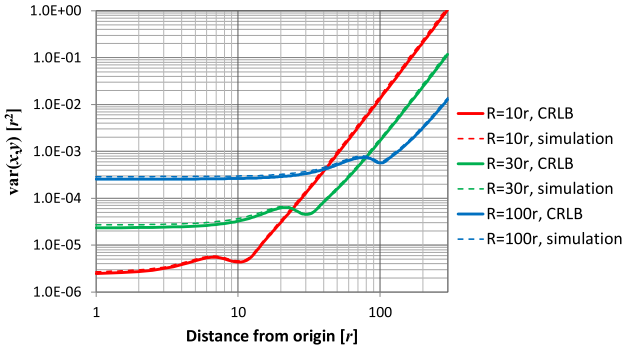

FIGURE 16. Cramer-Rao bound and variation of position estimation error in a system with $K = 3$ groups of transmitters, $M = 3$ transmitters in each group, $N = 3$ receivers in the mobile object. Measurement errors modeled by normal distribution with σ =0.001r.

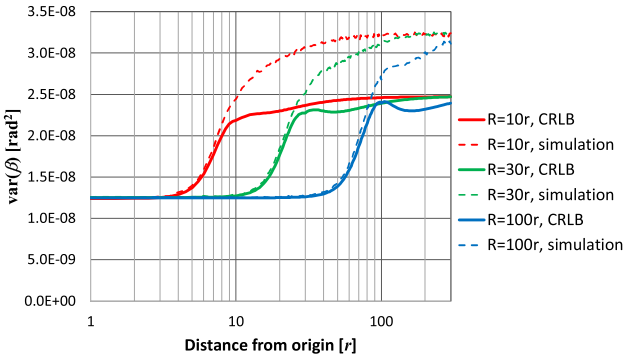

FIGURE 17. Cramer-Rao bound and variation of orientation angle estimation error in a system with $K = 3$ groups of transmitters, $M = 3$ transmitters in each group, $N = 3$ receivers in the mobile object. Measurement errors modeled by normal distribution with σ =0.001r.

results of the CRLB and variance of orientation angle estimation error. Both graphs were prepared under the assumption that the distance difference measurement errors are modeled by Gaussian distribution with a standard deviation of $0.001r$ but the simulations showed that the results obtained for other values, both higher and lower, are proportionately scaled without significant changes in the shape of the graphs.

Inside the area surrounded by groups of base stations (parts of the graphs at distances up to $10r$, $30r$ and $100r$ in Fig. 16), the possible quality of position estimation, indicated by the Cramer-Rao bound, shows limited variability in values, but outside this area, the CRLB values increase rapidly with the distance from the origin of the coordinate system in the center between groups of base stations. Although it is not clearly visible in Fig. 16 due to the logarithmic scale, the variance of the position estimation results obtained with the Gauss-Newton algorithm is only slightly higher than the CRLB, by 10 to 15 % over the entire range of simulated distances from the origin. Even better results can be observed for orientation estimation near the center of the area surrounded by groups of base stations, where the variance of the angle estimates is equal to the CRLB.

IV. CONCLUSION

This paper presents a method for simultaneous position and orientation estimation using time-difference measurements in a partially synchronous system. In the proposed solution, stationary base stations, which in this paper are assumed to be reference transmitters, are divided into groups, and the transmission of positioning signals is synchronized only within the group, while different groups operate asynchronously. The proposed system is an extension and generalization of the solution previously described by the same authors in [23], and the main assumption made during the study is that the synchronization problem of reference transmitters increases with the distance between them. Therefore, local synchronization of only closely located base stations should be much easier than global synchronization of all base stations in a wide area of system operation.

Possible application areas for the proposed system structure include aviation, as already mentioned in Section I, and marine navigation. It is worth noting that in both proposed application areas, the use of more than one device on the mobile object has a significant advantage. The orientation angle estimated with the proposed system will correspond to the aircraft or watercraft's heading, which is impossible to measure by the radio method using only one node on the tracked object [33], unlike the course angle, which can be easily estimated from a sequence of position estimates from any positioning system.

Future work may include checking the possibility of using the method of combining all TDOA measurements from unsynchronized network fragments in the proposed system, which was proposed in [34].

APPENDIX

By defining auxiliary variables:

$$A = x + x^0_{rn_1}\cos\beta + y^0_{rn_1}\sin\beta - x_{tm_1} \tag{A.1}$$
$$B = y + y^0_{rn_1}\cos\beta - x^0_{rn_1}\sin\beta - y_{tm_1} \tag{A.2}$$
$$C = x + x^0_{rn_2}\cos\beta + y^0_{rn_2}\sin\beta - x_{tm_2} \tag{A.3}$$
$$D = y + y^0_{rn_2}\cos\beta - x^0_{rn_2}\sin\beta - y_{tm_2} \tag{A.4}$$
$$E = x^0_{rn_1}\cos\beta + y^0_{rn_1}\sin\beta \tag{A.5}$$
$$F = y^0_{rn_1}\cos\beta - x^0_{rn_1}\sin\beta \tag{A.6}$$
$$G = x^0_{rn_2}\cos\beta + y^0_{rn_2}\sin\beta \tag{A.7}$$
$$H = y^0_{rn_2}\cos\beta - x^0_{rn_2}\sin\beta \tag{A.8}$$

the partial derivatives of log-likelihood function $\ln p(\boldsymbol{\rho};\boldsymbol{\theta})$ for the Fisher information matrix $\mathbf{I}(\boldsymbol{\theta})$ can be written in simplified form as presented in A.9–A.17.

After calculating the expected value with respect to the measurement results $d_{m_2,n_2} - d_{m_1,n_1}$, the expression $\left(d_{m2,n2} - d_{m_1,n_1}\right) - \left(\sqrt{C^2+D^2} - \sqrt{A^2+B^2}\right)$ takes a zero value. Therefore, the components of the Fisher information matrix are simplified to the first part from the formulas (A.9)–(A.17), as shown at the top of the next page, only.

$$\frac{\partial^2 \ln p(\boldsymbol{\rho};\boldsymbol{\theta})}{\partial x^2} = -\frac{1}{\sigma^2}\sum_{m_1,m_2,n_1,n_2}\left\{\left(\frac{A}{\sqrt{A^2+B^2}}-\frac{C}{\sqrt{C^2+D^2}}\right)^2+\left(\frac{-1}{\sqrt{C^2+D^2}}+\frac{C^2}{\left(C^2+D^2\right)^{\frac{3}{2}}}+\frac{1}{\sqrt{A^2+B^2}}-\frac{A^2}{\left(A^2+B^2\right)^{\frac{3}{2}}}\right)\cdot\left(\left(d_{m_2,n_2}-d_{m_1,n_1}\right)-\left(\sqrt{C^2+D^2}-\sqrt{A^2+B^2}\right)\right)\right\} \tag{A.9}$$

$$\frac{\partial^2 \ln p(\boldsymbol{\rho};\boldsymbol{\theta})}{\partial x\partial y} = -\frac{1}{\sigma^2}\sum_{m_1,m_2,n_1,n_2}\left\{\left(\frac{A}{\sqrt{A^2+B^2}}-\frac{C}{\sqrt{C^2+D^2}}\right)\cdot\left(\frac{B}{\sqrt{A^2+B^2}}-\frac{D}{\sqrt{C^2+D^2}}\right)+\left(\frac{CD}{\left(C^2+D^2\right)^{\frac{3}{2}}}-\frac{AB}{\left(A^2+B^2\right)^{\frac{3}{2}}}\right)\cdot\left(\left(d_{m_2,n_2}-d_{m_1,n_1}\right)-\left(\sqrt{C^2+D^2}-\sqrt{A^2+B^2}\right)\right)\right\} \tag{A.10}$$

$$\frac{\partial^2 \ln p(\boldsymbol{\rho};\boldsymbol{\theta})}{\partial x\partial \beta} = -\frac{1}{\sigma^2}\sum_{m_1,m_2,n_1,n_2}\left\{\left(\frac{A}{\sqrt{A^2+B^2}}-\frac{C}{\sqrt{C^2+D^2}}\right)\cdot\left(\frac{FA-BE}{\sqrt{A^2+B^2}}-\frac{HC-GD}{\sqrt{C^2+D^2}}\right)+\left(\frac{-H}{\sqrt{C^2+D^2}}+\frac{C\left(CH-DG\right)}{\left(C^2+D^2\right)^{\frac{3}{2}}}+\frac{F}{\sqrt{A^2+B^2}}-\frac{A\left(FA-BE\right)}{\left(A^2+B^2\right)^{\frac{3}{2}}}\right)\cdot\left(\left(d_{m_2,n_2}-d_{m_1,n_1}\right)-\left(\sqrt{C^2+D^2}-\sqrt{A^2+B^2}\right)\right)\right\} \tag{A.11}$$

$$\frac{\partial^2 \ln p(\boldsymbol{\rho};\boldsymbol{\theta})}{\partial y\partial x} = \frac{\partial^2 \ln p(\boldsymbol{\rho};\boldsymbol{\theta})}{\partial x\partial y} \tag{A.12}$$

$$\frac{\partial^2 \ln p(\boldsymbol{\rho};\boldsymbol{\theta})}{\partial y^2} = -\frac{1}{\sigma^2}\sum_{m_1,m_2,n_1,n_2}\left\{\left(\frac{B}{\sqrt{A^2+B^2}}-\frac{D}{\sqrt{C^2+D^2}}\right)^2+\left(\frac{-1}{\sqrt{C^2+D^2}}+\frac{D^2}{\left(C^2+D^2\right)^{\frac{3}{2}}}+\frac{1}{\sqrt{A^2+B^2}}-\frac{B^2}{\left(A^2+B^2\right)^{\frac{3}{2}}}\right)\cdot\left(\left(d_{m_2,n_2}-d_{m_1,n_1}\right)-\left(\sqrt{C^2+D^2}-\sqrt{A^2+B^2}\right)\right)\right\} \tag{A.13}$$

$$\frac{\partial^2 \ln p(\boldsymbol{\rho};\boldsymbol{\theta})}{\partial y\partial \beta} = -\frac{1}{\sigma^2}\sum_{m_1,m_2,n_1,n_2}\left\{\left(\frac{B}{\sqrt{A^2+B^2}}-\frac{D}{\sqrt{C^2+D^2}}\right)\cdot\left(\frac{FA-BE}{\sqrt{A^2+B^2}}-\frac{HC-GD}{\sqrt{C^2+D^2}}\right)+\left(\frac{G}{\sqrt{C^2+D^2}}+\frac{D\left(CH-DG\right)}{\left(C^2+D^2\right)^{\frac{3}{2}}}-\frac{E}{\sqrt{A^2+B^2}}-\frac{B\left(FA-BE\right)}{\left(A^2+B^2\right)^{\frac{3}{2}}}\right)\cdot\left(\left(d_{m_2,n_2}-d_{m_1,n_1}\right)-\left(\sqrt{C^2+D^2}-\sqrt{A^2+B^2}\right)\right)\right\} \tag{A.14}$$

$$\frac{\partial^2 \ln p(\boldsymbol{\rho};\boldsymbol{\theta})}{\partial \beta\partial x} = \frac{\partial^2 \ln p(\boldsymbol{\rho};\boldsymbol{\theta})}{\partial x\partial \beta} \tag{A.15}$$

$$\frac{\partial^2 \ln p(\boldsymbol{\rho};\boldsymbol{\theta})}{\partial \beta\partial y} = \frac{\partial^2 \ln p(\boldsymbol{\rho};\boldsymbol{\theta})}{\partial y\partial \beta} \tag{A.16}$$

$$\frac{\partial^2 \ln p(\boldsymbol{\rho};\theta)}{\partial \beta^2} = -\frac{1}{\sigma^2}\sum_{m_1,m_2,n_1,n_2}\left\{\left(\frac{FA-EB}{\sqrt{A^2+B^2}}-\frac{HC-GD}{\sqrt{C^2+D^2}}\right)^2+\left(-\frac{G^2+H^2-GC-HD}{\sqrt{C^2+D^2}}+\frac{(HC-GD)^2}{\left(C^2+D^2\right)^{\frac{3}{2}}}+\frac{E^2+F^2-EA-FB}{\sqrt{A^2+B^2}}-\frac{(FA-EB)^2}{\left(A^2+B^2\right)^{\frac{3}{2}}}\right)\cdot\left(\left(d_{m_2,n_2}-d_{m_1,n_1}\right)-\left(\sqrt{C^2+D^2}-\sqrt{A^2+B^2}\right)\right)\right\} \tag{A.17}$$

REFERENCES

[1] S. Ghorpade, M. Zennaro, and B. Chaudhari, "Survey of localization for Internet of Things nodes: Approaches, challenges and open issues," *Future Internet*, vol. 13, no. 8, p. 210, Aug. 2021, doi: 10.3390/fi13080210.

[2] C. Laoudias, A. Moreira, S. Kim, S. Lee, L. Wirola, and C. Fischione, "A survey of enabling technologies for network localization, tracking, and navigation," *IEEE Commun. Surveys Tuts.*, vol. 20, no. 4, pp. 3607–3644, 4th Quart., 2018, doi: 10.1109/COMST.2018.2855063.

[3] H. Khan, M. N. Hayat, and Z. U. Rehman, "Wireless sensor networks free-range base localization schemes: A comprehensive survey," in *Proc. Int. Conf. Commun., Comput. Digit. Syst. (C-CODE)*, Islamabad, Pakistan, Mar. 2017, pp. 144–147, doi: 10.1109/C-CODE.2017.7918918.

[4] A. Dwivedi and P. R. Vamsi, "Performance analysis of range free localization methods for wireless sensor networks," in *Proc. 4th Int. Conf. Signal Process., Comput. Control (ISPCC)*, Solan, India, Sep. 2017, pp. 521–526, doi: 10.1109/ispcc.2017.8269734.

[5] S. Sivasakthiselvan and V. Nagarajan, "Localization techniques of wireless sensor networks: A review," in *Proc. Int. Conf. Commun. Signal Process. (ICCSP)*, Chennai, India, Jul. 2020, pp. 1643–1648, doi: 10.1109/ICCSP48568.2020.9182290.

[6] M. A. Al-Ammar, S. Alhadhrami, A. Al-Salman, A. Alarifi, H. S. Al-Khalifa, A. Alnafessah, and M. Alsaleh, "Comparative survey of indoor positioning technologies, techniques, and algorithms," in *Proc. Int. Conf. Cyberworlds*, Santander, Spain, Oct. 2014, pp. 245–252, doi: 10.1109/CW.2014.41.

[7] S. He, "Asynchronous time difference of arrival positioning system and implementation," Ph.D. dissertation, Dept. Elect. Comput. Eng., Univ. Victoria, Victoria, BC, Canada, 2016.
[8] S. He and X. Dong, "High-accuracy localization platform using asynchronous time difference of arrival technology," *IEEE Trans. Instrum. Meas.*, vol. 66, no. 7, pp. 1728–1742, Jul. 2017, doi: 10.1109/TIM.2017.2666278.
[9] F. Bandiera, A. Coluccia, G. Ricci, F. Ricciato, and D. Spano, "TDOA localization in asynchronous WSNs," in *Proc. 12th IEEE Int. Conf. Embedded Ubiquitous Comput.*, Milan, Italy, Aug. 2014, pp. 193–196, doi: 10.1109/EUC.2014.35.
[10] B. Xu, G. Sun, R. Yu, and Z. Yang, "High-accuracy TDOA-based localization without time synchronization," *IEEE Trans. Parallel Distrib. Syst.*, vol. 24, no. 8, pp. 1567–1576, Aug. 2013, doi: 10.1109/TPDS.2012.248.
[11] F. Ma, Z.-M. Liu, and F. Guo, "Direct position determination in asynchronous sensor networks," *IEEE Trans. Veh. Technol.*, vol. 68, no. 9, pp. 8790–8803, Sep. 2019, doi: 10.1109/TVT.2019.2928638.
[12] J. Zhou, L. Shen, and Z. Sun, "A new method of D-TDOA time measurement based on RTT," in *Proc. MATEC Web Conf.*, 2018, pp. 1–5, doi: 10.1051/matecconf/201820703018.
[13] A. Vashistha, R. W. C. Ling, and L. L. Choi, "A TDOA measurement technique for asynchronous indoor localization system using UWB-IR," in *Proc. Int. Conf. Indoor Positioning Indoor Navigat. (IPIN)*, 2016, pp. 1–5.
[14] L. Song, H. Zou, and T. Zhang, "A low complexity asynchronous UWB TDOA localization method," *Int. J. Distrib. Sensor Netw.*, vol. 2015, no. 10, pp. 1–9, 2015, doi: 10.1155/2015/675490.
[15] B. Malcic, S. Sajic, M. Trifunovic, and V. Jovanovic, "Asynchronous 2D-TDOA localization method," in *Proc. 29th Telecommun. Forum (TELFOR)*, Belgrade, Serbia, Nov. 2021, pp. 1–4, doi: 10.1109/TELFOR52709.2021.9653271.
[16] X. Zhao and B. Zhu, "Vehicle positioning and navigation in asynchronous navigation system," *Actuators*, vol. 11, no. 2, p. 54, Feb. 2022, doi: 10.3390/act11020054.
[17] R. M. Vaghefi and R. M. Buehrer, "Asynchronous time-of-arrival-based source localization," in *Proc. IEEE Int. Conf. Acoust., Speech Signal Process.*, Vancouver, BC, Canada, May 2013, pp. 4086–4090, doi: 10.1109/ICASSP.2013.6638427.
[18] H. H. Fan and C. Yan, "Asynchronous differential TDOA for sensor self-localization," in *Proc. IEEE Int. Conf. Acoust., Speech Signal Process. (ICASSP)*, Honolulu, HI, USA, Apr. 2007, pp. II-1109–II-1112, doi: 10.1109/icassp.2007.366434.
[19] W. Zheng and N. González-Prelcic, "Joint position, orientation AND channel estimation in hybrid mmWAVE MIMO systems," in *Proc. 53rd Asilomar Conf. Signals, Syst., Comput.*, Pacific Grove, CA, USA, Nov. 2019, pp. 1453–1458, doi: 10.1109/IEEECONF44664.2019.9048769.
[20] A. Shahmansoori, G. E. Garcia, G. Destino, G. Seco-Granados, and H. Wymeersch, "5G position and orientation estimation through millimeter wave MIMO," in *Proc. IEEE Globecom Workshops (GC Wkshps)*, San Diego, CA, USA, Dec. 2015, pp. 1–6, doi: 10.1109/GLOCOMW.2015.7413967.
[21] E.-J. Theussl, D. Ninevski, and P. O'Leary, "Measurement of relative position and orientation using UWB," in *Proc. IEEE Int. Instrum. Meas. Technol. Conf. (IMTC)*, Auckland, New Zealand, May 2019, pp. 1–6, doi: 10.1109/I2MTC.2019.8827149.
[22] A. Fishberg and J. P. How, "Multi-agent relative pose estimation with UWB and constrained communications," in *Proc. IEEE/RSJ Int. Conf. Intell. Robots Syst. (IROS)*, Kyoto, Japan, Oct. 2022, pp. 778–785, doi: 10.1109/IROS47612.2022.9982005.
[23] J. Stefanski and J. Sadowski, "Asynchronous method of simultaneous object position and orientation estimation with two transmitters," *Navigation, J. Inst. Navigat.*, vol. 70, no. 4, 2023, Art. no. navi.601, doi: 10.33012/navi.601.
[24] W. Foy, "Position-location solutions by Taylor-series estimation," *IEEE Trans. Aerosp. Electron. Syst.*, vol. AES-12, no. 2, pp. 187–194, Mar. 1976, doi: 10.1109/taes.1976.308294.
[25] C. Mensing and S. Plass, "Positioning algorithms for cellular networks using TDOA," in *Proc. IEEE Int. Conf. Acoust. Speech Signal Process.*, Toulouse, France, May 2006, p. 4, doi: 10.1109/ICASSP.2006.1661018.
[26] J. B. Y. Tsui, *Fundamentals of Global Positioning System Receivers. A Software Approach*. Hoboken, NJ, USA: Wiley, 2000.
[27] S. Joardar, T. A. Siddique, S. Alam, and M. Hossam-E-Haider, "Analyses of different types of errors for better precision in GNSS," in *Proc. 3rd Int. Conf. Electr. Eng. Inf. Commun. Technol. (ICEEICT)*, Dhaka, Bangladesh, Sep. 2016, pp. 1–6, doi: 10.1109/CEEICT.2016.7873127.
[28] M. Tahsin, S. Sultana, T. Reza, and M. Hossam-E-Haider, "Analysis of DOP and its preciseness in GNSS position estimation," in *Proc. Int. Conf. Electr. Eng. Inf. Commun. Technol. (ICEEICT)*, Savar, Bangladesh, May 2015, pp. 1–6, doi: 10.1109/ICEEICT.2015.7307445.
[29] K. Bronk and J. Stefanski, "Bad geometry influence on positioning accuracy in wireless networks," in *Proc. Int. Conf. Comput. Tool (EUROCON)*, Warsaw, Poland, 2007, pp. 1131–1135, doi: 10.1109/eurcon.2007.4400257.
[30] J. D. Bard and F. M. Ham, "Time difference of arrival dilution of precision and applications," *IEEE Trans. Signal Process.*, vol. 47, no. 2, pp. 521–523, Feb. 1999, doi: 10.1109/78.740135.
[31] D. Torrieri, "Statistical theory of passive location systems," *IEEE Trans. Aerosp. Electron. Syst.*, vol. AES-20, no. 2, pp. 183–198, Mar. 1984, doi: 10.1109/taes.1984.310439.
[32] S. M. Kay, *Fundamentals of Statistical Signal Processing: Estimation Theory*. Upper Saddle River, NJ, USA: Prentice-Hall, 1993.
[33] E. B. Kalveland, "Estimation of orientation of an aircraft using position data only," Norwegian Defence Res. Establishment, Kjeller, Norway, FFI Rep. 22/01379, 2022.
[34] C. Gioia, F. Sermi, and D. Tarchi, "Multi-network asynchronous TDOA algorithm test in a simulated maritime scenario," *Sensors*, vol. 20, no. 7, p. 1842, Mar. 2020, doi: 10.3390/s20071842.

JAROSLAW SADOWSKI received the M.Sc. degree in mobile radio communication systems from the Gdańsk University of Technology, Gdańsk, Poland, in 2002, the Ph.D. degree in radio communication, in 2010, and the D.Sc. degree in informatics and telecommunications, in 2019.

From 2002 to 2006, he worked in the industry designing and constructing 2G/3G base stations. Since 2007, he has been an Assistant Professor with the Department of Radio Communication Systems and Networks (DRCSN), Gdańsk University of Technology. Since 2018, he has been the Deputy Head of the Department of Radio Communication Systems and Networks, Gdańsk University of Technology, where he has been the Head, since 2020. His research interests include localization in indoor environments, ultra-wideband technology, and electromagnetic compatibility. He is a member of the EMC Section of the Committee on Electronics and Telecommunication of the Polish Academy of Sciences.

JACEK STEFANSKI (Member, IEEE) received the M.Sc., Ph.D., and D.Sc. degrees in telecommunications engineering from the Gdańsk University of Technology (GUT), Poland, in 1993, 2000, and 2012, respectively.

From 1993 to 2000, he was an Assistant Professor with the Department of Radio Communication Systems and Networks (DRCSN), GUT. Since 2001, he has been an Associate Professor with DRCSN. From 2005 to 2009, he was an Assistant Professor with the National Institute of Telecommunications, Gdansk Branch. Since 2020, he has been the Dean of the Faculty of Electronics, Telecommunications and Informatics, GUT. He is the author or coauthor of more than 350 articles. He is the coauthor of 12 patents and over a dozen patent applications. His research interests include analysis, simulation, design and measurement of cellular, wireless and trunked radio systems, digital modulation techniques, channel coding, signal spreading, radio signal reception, measurement of radio wave propagation, field strength prediction, software radio design, location services, ad-hoc sensor networks, radio monitoring systems, and radio navigation systems. He is a member of the Electromagnetic Compatibility Section of the Electronics and Telecommunications Committee of the Polish Academy of Sciences and the Sub-Committee on Navigation, Communications and Search and Rescue (NCSR) in the International Maritime Organization (IMO). He is also a member of the Board of Associate Editors of the *International Journal of Electronics and Telecommunications*.